

Fast Bound Pool Fraction Imaging of the In Vivo Rat Brain: Association with Myelin Content and Validation in the C6 Glioma Model

H. R. Underhill¹, R. C. Rostomily¹, A. M. Mikheev¹, C. Yuan¹, and V. L. Yarnykh¹

¹University of Washington, Seattle, WA, United States

Introduction: Cross-relaxation imaging (CRI)¹ is a method for quantitative mapping of the parameters describing the kinetics of magnetization transfer (MT) between mobile water protons (free pool) and macromolecular protons (bound pool) based on the two-pool model.² While all parameters of the two-pool model (specifically, the bound pool fraction f , the rate constant k , and the transverse relaxation times of the free and bound pools T_2^F and T_2^B) can be determined using an appropriate CRI experimental design with a sufficiently large number of measurements,^{3,4} recent studies have been focused on the development of faster acquisition techniques allowing determination of subsets of two-pool model parameters from a limited number of experimental points based on certain theoretical approximations.^{1,4-8} One of these parameters, the bound pool fraction f is of special interest, since it provides direct measurement of the portion of macromolecular protons causing the MT effect and is indicative of the total content of macromolecules in tissues. CRI has demonstrated a strong correspondence between f and major fiber tracts in the human brain *in vivo*¹. Recently, a time-efficient methodology for single-parameter bound pool fraction mapping from two off-resonance MT measurements has been proposed^{7,8} based on constraining other model parameters (specifically, T_2^B , the product $T_2^F R_1^F$, and the inverse rate constant $k(1-f)/f$) with their average-brain values. While this approach has a good clinical perspective due to fast acquisition and high quality of resulting f maps, it has not been validated in the context of the effects of parameter constraints and histological correlations of observed f values. In this study, we first aimed to determine associations between the bound pool fraction obtained by either the full two-pool model fit or the fast single-parameter method^{7,8} and key histology features (myelin density, axonal content, and cellularity) in the normal rat brain and C6 glioma model *in vivo*. Second, we sought to identify optimal parameter constraints for the fast f mapping method^{7,8} and characterize its accuracy for brain imaging at 3.0 T.

Methods: MRI protocol: Five healthy adult male rats were imaged and four adult male rats were imaged two weeks after intracranial inoculation with C6 cells. Rats were anesthetized with isoflurane and imaged on a 3.0 T Philips Achieva whole-body scanner (Philips, Best, Netherlands) with a T/R head coil for RF transmission and an in-house built combined solenoid-surface coil⁹ for RF reception. Fifteen pulsed Z-spectroscopic data points with variable offset frequencies (Δ) of the off-resonance saturation pulse ($\Delta = 0.6, 1, 2, 4$, and 8 kHz; duration 18 ms) and effective flip angles of 650°, 800°, and 950° were acquired with a 3D spoiled gradient echo pulse sequence (TR/TE = 42/4.6 ms, $\alpha = 10^\circ$) as previously described.^{1,4} A reference image for data normalization was obtained with $\Delta = 96$ kHz (no MT effect is observed at this frequency) for each effective flip angle to ensure that the transmitter operated with identical gain settings. A complementary R_1 map necessary for parameter fitting was obtained using the variable flip angle (VFA) method with a 3D spoiled gradient echo sequence (TR/TE = 20/2.3 ms, $\alpha = 4, 10, 20$, and 40°). All Z-spectroscopic and VFA images were acquired with FOV = 29×29×19.8 mm, matrix = 97×97×66, resolution 0.3×0.3×0.3 mm (zero-interpolated to 0.15×0.15×0.15 mm). Scan time per excitation was 4.4 minutes and 2.1 minutes per point for Z-spectroscopy and VFA, respectively. Whole-brain B_0 and B_1 maps were acquired to establish actual off-resonance of the saturation pulse and determine actual flip angles during parameter fitting as previously described.⁴ Total scan time for all images was 111.4 minutes. **Image analysis:** ROIs from within a total of nine gray matter (GM) and white matter (WM) structures were used for four-parameter fitting (k, f, T_2^F , and T_2^B) of 15-pt data. Identical ROIs were used for one-parameter fitting (f) using 2-pt data (950°; $\Delta = 4$ and 8 kHz) and constraints for other parameters derived from the four-parameter fit. Myelin density, axon content, and cellularity were determined from corresponding anatomic structures on histology sections stained with Luxol-Fast blue, Bielchowsky's silver impregnation, and hematoxylin & eosin, respectively. Pearson's correlation coefficient, r , was used to compare CRI parameters to histology and to compare f derived from four- and single-parameter fittings. Simulation-based error analysis using an established model of CRI¹ was done to determine effects of constraints derived from normal tissues on one-parameter fitting of normal and pathologic tissue data similar to the earlier publication.⁴ Bound pool fraction values derived from four-parameter and one-parameter fits were subsequently compared.

Results: Histology validation: The bound pool fraction derived from the four-parameter fit was strongly associated with myelin density ($r = 0.99$, $p < 0.001$), which persisted in separate analyses of GM ($r = 0.89$, $p = 0.046$) and WM ($r = 0.97$, $p = 0.029$). Similarly, there was a strong association between 2-pt, single-parameter fit of f and myelin density in all normal brain tissues ($r = 0.99$, $p < 0.001$), and separately in GM ($r = 0.91$, $p = 0.030$) and WM ($r = 0.95$, $p = 0.047$). The regression equation defining the association between f and myelin density ($MD; f = 0.21 \times MD + 3.9$) was used to construct whole-brain myelin maps (Figure 1). In brains with tumor present, effects of tumor infiltration were visualized on f -maps and myelin maps (Figure 2). Significant associations with f were not identified for the other histology parameters nor were other CRI parameters significantly associated with histology.

Accuracy of fast f mapping: The mean values from non-tumor tissues of T_2^B , the product $T_2^F R_1^F$, and the constant $k(1-f)/f$ determined for single-parameter fitting were 10.7 μ s, 0.030, and 29 s^{-1} , respectively. Comparing ROI-based results in non-tumor tissue from 15-pt, four-parameter fit and the 2-pt, single-parameter fit of f yielded strong associations across all structures ($r = 0.996$, $p < 0.001$), as well as separately within GM ($r = 0.98$, $p = 0.003$) and within WM ($r = 0.97$, $p = 0.031$). Errors consequent of parameter constraints in WM, GM, and tumor from simulations were <10%. A comparison of values for f between four- and single-parameter fit for *in vivo* rat brain gliomas was within this expected margin ($N=4$; mean±SE; 3.9±0.2% vs. 4.0±0.2%, respectively).

Conclusion: The bound pool fraction obtainable with *in vivo*, whole-brain CRI in the rat at 3.0 T primarily corresponds to myelin density. A time-efficient acquisition directed at solely acquiring the bound pool fraction yields a similar correspondence with myelin density without substantial errors in the estimation of f induced by the application of a constrained parametric model. The improved time-efficiency may enable improvements in resolution, SNR, or both. The *in vivo* whole-brain bound pool fraction maps and myelin density maps identified changes in both GM and WM associated with the presence of a tumor. Bound pool fraction imaging and myelin density maps may be beneficial in clinical and animal studies aimed at detecting and monitoring neurological diseases that affect GM, WM, or both.

References: 1. Yarnykh *NeuroImage* 2004;23:409-24 2. Henkelman *MRM* 1993;29:759-66 3. Sled *MRM* 2001; 46:923-31 4. Underhill *NeuroImage* 2009;47:1568-78 5. Ropele *MRM* 2003;49:864-71 6. Gloor *MRM* 2008;60:691-700 7. Underhill *Proc. ISMRM* 2010;30:00.8. Yarnykh *Proc. ISMRM* 2010;43:42 9. Underhill *MRM* 2010;64:883-892

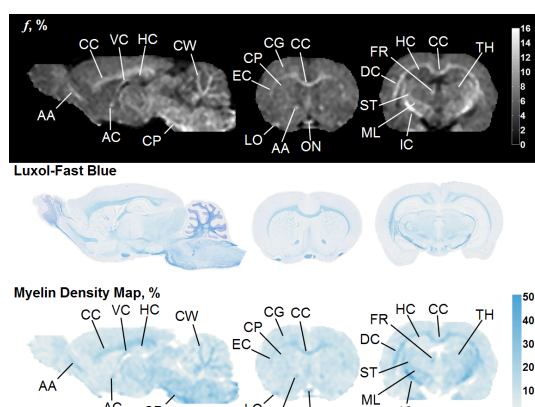


Figure 1. Bound pool fraction maps (top row), Luxol-Fast Blue stain (middle row), and myelin maps (bottom row) of a normal rat brain. AA = anterior limb; anterior commissure; AC=anterior commissure; CC=cortex callosum; CG=cortical gray matter; CP=cerebral peduncle; CW=cerebellar white matter; DC=deep cerebral white matter; EC=external capsule; FR=fasciculus retroflexus; HC=hippocampus; IC=internal capsule; LO=lateral olfactory tract; ML=medial lemniscus; ON=optic nerve; ST=superior thalamic radiations; TH=thalamus; VC=ventral hippocampal commissure

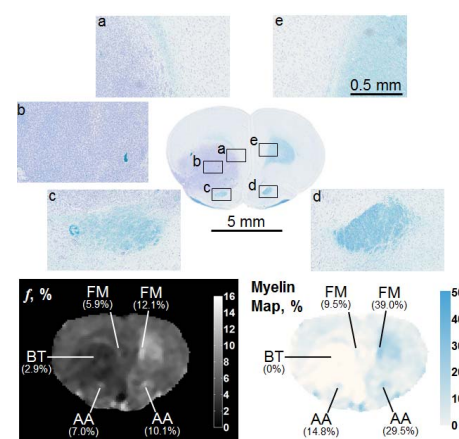


Figure 2. Bulk tumor (BT, b) is characterized by a very low f and myelin density. The tumor is also affecting WM density adjacent to growth. The fimbria minor (FM) and the anterior limb of the anterior commissure (AA) are less dense adjacent to the tumor (a and c, respectively) compared to the contralateral side (d and e, respectively).